EARTHQUAKE ENGINEERING AND STRUCTURAL DYNAMICS
Earthquake Engng Struct. Dyn. 2003; **32**:1603–1626 (DOI: 10.1002/eqe.291)

A simplified method of constructing fragility curves for highway bridges

Kazi R. Karim*,† and Fumio Yamazaki

Institute of Industrial Science, The University of Tokyo, 4-6-1 Komaba, Meguro-ku, Tokyo 153-8505, Japan

SUMMARY

Fragility curves are found to be useful tools for predicting the extent of probable damage. They show the probability of highway structure damage as a function of strong motion parameters, and they allow the estimation of a level of damage probability for a known ground motion index. In this study, an analytical approach was adopted to develop the fragility curves for highway bridges based on numerical simulation. Four typical RC bridge piers and two RC bridge structures were considered, of which one was a non-isolated system and the other was an isolated system, and they were designed according to the seismic design code in Japan. From a total of 250 strong motion records, selected from Japan, the United States, and Taiwan, non-linear time history analyses were performed, and the damage indices for the bridge structures were obtained. Using the damage indices and ground motion parameters, fragility curves for the four bridge piers and the two bridge structures were constructed assuming a lognormal distribution. It was found that there was a significant effect on the fragility curves due to the variation of structural parameters. The relationship between the fragility curve parameters and the over-strength ratio of the structures was also obtained by performing a linear regression analysis. It was observed that the fragility curve parameters showed a strong correlation with the over-strength ratio of the structures. Based on the observed correlation between the fragility curve parameters and the over-strength ratio of the structures, a simplified method was developed to construct the fragility curves for highway bridges using 30 non-isolated bridge models. The simplified method may be a very useful tool to construct the fragility curves for non-isolated highway bridges in Japan, which fall within the same group and have similar characteristics. Copyright © 2003 John Wiley & Sons, Ltd.

KEY WORDS: strong motion records; ground motion indices; highway bridges; damage analysis; regression model; fragility curves

INTRODUCTION

The actual damage [1, 2] to highway systems from recent earthquakes has emphasized the need for risk assessment of the existing highway transportation systems. The vulnerability assessment of bridges is useful for seismic retrofitting decisions, disaster response planning,

* Correspondence to: Kazi R. Karim, Institute of Industrial Science, The University of Tokyo, 4-6-1 Komaba, Meguro-ku, Tokyo 153-8505, Japan.
† E-mail: kazi@ares.iis.u-tokyo.ac.jp

Received 14 March 2002
Revised 19 October 2002
Accepted 25 November 2002

estimation of direct monetary loss, and evaluation of loss of functionality of highway systems. Hence, it is important to know the degree of damage [1, 3, 4] to the highway bridge structures due to earthquakes. To estimate a damage level (slight, moderate, extensive, and complete) for highway bridge structures, fragility curves [1–3, 5] are found to be a useful tool. Fragility curves show the relationship between the probability of highway structure damage and the ground motion indices. They allow the estimation of a damage level for a known ground motion index.

The 1995 Kobe earthquake, which is considered to be one of the most damaging earthquakes in Japan, caused severe damage to expressway structures in the Kobe area. Based on the actual damage data from the earthquake, a set of empirical fragility curves [1] was constructed. The empirical fragility curves give a general idea about the relationship between the damage levels of the highway structures and the ground motion indices. These fragility curves may be used for damage estimation of highway bridge structures in Japan. However, the empirical fragility curves do not specify the type of structure, structural performance (static and dynamic) or variation of input ground motion, and may not be applicable for estimating the level of damage probability for specific bridge structures [5]. It is assumed that structural parameters and input motion characteristics (e.g., frequency contents, phase, and duration) have an influence on the damage to the structure for which there will be an effect on the fragility curves. Karim and Yamazaki [6] developed a set of analytical fragility curves for highway bridge piers considering the variation of input ground motions based on numerical simulation, and found that there is a significant effect of earthquake ground motions on fragility curves.

The objective of this study is to develop analytical fragility curves for highway bridges considering the variation of structural parameters based on numerical simulation. Four typical RC bridge piers [7] and two RC bridge structures are considered (of which one is a non-isolated system and the other one is an isolated system), and they are designed [8, 9] according to the seismic design code [10] in Japan. A total of 250 strong motion records were selected from Japan, the United States, and Taiwan as the input motions. Using the selected input motions, damage analyses of the bridge structures are performed, and the fragility curves are obtained assuming a lognormal distribution [1, 11]. Based on the observed correlation between the fragility curve parameters and the over-strength ratio of the structures, a simplified method is developed to construct the fragility curves using 30 non-isolated bridge models. The simplified method may be a very useful tool to construct the fragility curves for non-isolated highway bridges in Japan, which fall within the same group and have similar characteristics.

DEVELOPMENT OF FRAGILITY CURVES

Empirical fragility curves

Yamazaki *et al.* [1] developed a set of empirical fragility curves based on the actual damage data from the 1995 Kobe earthquake, and shown the relationship between the damage that occurred to the expressway bridge structures and the ground motion indices. The approach employed to construct the empirical fragility curves is briefly described here while the details of the approach can be found elsewhere [1]. In this approach, the damage data of the JH expressway structures due to the Kobe earthquake were collected, and the ground motion

indices along the expressways were estimated based on the estimated strong motion distribution using the Kriging technique. The damage data and ground motion indices were related to each damage rank [1, 3, 4], and the damage ratio for each damage rank was obtained. Finally, using the damage ratio for each damage rank, the empirical fragility curves for the expressway bridge structures were constructed assuming a lognormal distribution [11].

Analytical fragility curves

Karim and Yamazaki [6] developed a set of analytical fragility curves for highway bridge piers based on numerical simulation and considering the variation of input ground motions. The procedures adopted to construct the analytical fragility curves are briefly described here, while for the details of the procedures one should go through Reference [6]. In this approach, first the non-linear static pushover analysis of the structure is performed, which includes the shear vs. strain and moment vs. curvature analyses of the cross-sections (it is recommended in the code [10] that a pier should be divided at least into 50 slices), and the force-displacement relationship at the top of the bridge pier is obtained by using the shear vs. strain and moment vs. curvature relationships of all cross-sections. Using the elastic stiffness (obtained from the force-displacement relationship), the non-linear dynamic response analyses are performed for the selected input ground motions, which were normalized to different excitation levels. The damage to the structure (pier) is then quantified by a damage index (DI) that is obtained by using a damage model and the number of occurrences of a particular damage rank is counted by calibrating the damage indices in different excitation levels, which is then used to obtain the damage ratio of each damage rank in each excitation level. The damage ratio is then plotted on a lognormal probability scale from where the two parameters of the fragility curves, i.e., mean and standard deviation, are obtained by performing a linear regression analysis. Finally, the fragility curves are constructed for each damage rank with respect to the ground motion indices using the obtained mean and standard deviation. The procedures adopted for constructing the analytical fragility curves can be summarized as follows:

1. Selection of the earthquake ground motion records.
2. Normalization of Peak Ground Acceleration (PGA) of the selected records to different excitation levels.
3. Making a physical model of the structure.
4. Performing a non-linear static pushover analysis and obtaining the elastic stiffness of the structure.
5. Selection of a hysteretic model for the non-linear dynamic response analysis.
6. Performing the non-linear dynamic response analysis using the elastic stiffness and the selected records.
7. Obtaining the damage indices of the structure in each excitation level using a damage model.
8. Calibration of the damage indices for each damage rank to obtain the damage ratio in each excitation level.
9. Plotting the damage ratio in each excitation level on a lognormal probability scale and obtaining the mean and standard deviation of the fragility curves for each damage rank by performing a linear regression analysis.

10. Construction of the fragility curves using the obtained mean and standard deviation with respect to the ground motion indices for each damage rank assuming a lognormal distribution.

PIER AND BRIDGE MODELS

Pier models

Four typical RC bridge piers [7] and two RC bridge structures are considered (of which one is a non-isolated system and the other is an isolated system). The piers are designed [8, 9] according to the 1964, 1980, 1990, and 1995 seismic design codes [10] assuming that only the size and reinforcement of the piers can be changed with other conditions such as the height of substructure (11.8 m), length (35 m) and weight of superstructure (23627 kN), ground condition (type II), and nominal design strength of concrete (14.7 MPa) and reinforcement (294 MPa) being unchanged.

The elevation and cross-sections of the four piers are shown in Figure 1. Based on past earthquake experience, the code requirements have been changed since 1964. One can see (Figure 1(b)) that the cross-sections as well as the amount of both longitudinal and tie reinforcements have been changed significantly from the 1964 code to the 1980 code. One can also see (Figure 1(b)) that the arrangement of tie reinforcement has also been changed significantly from the 1964 code to the 1980 code. These changes have been adopted in order to give better performance of the structure against an earthquake force. However, from 1990, it can be seen that the changes are not so significant. The longitudinal reinforcement (area ratio) for the four bridge piers is taken as 1.21%, 1.25%, 1.30%, and 1.36%, respectively, while the tie reinforcement (volumetric ratio) is taken as 0.09%, 0.32%, 0.64%, and 1.03%, respectively.

Bridge models

In the case of the two bridge models, they were designed according to the seismic design code in Japan [10] assuming that the size and reinforcement of the piers, height of the substructure, length and weight (W) of the superstructure, ground condition, and nominal design strength of concrete and reinforcement were unchanged. Note that the parametric values for the two bridge systems are taken as those of the 1980 pier except for the height, which is taken as 12 m. For the non-isolated bridge system, it is assumed that it has four spans with a 35 m span length having 675 kN/m superstructure weight, the piers are rectangular, pin-jointed to the superstructure and fixed to the base, and the superstructure is assumed to slide on ordinary frictionless bearings at the abutments.

For the isolated bridge system, a lead-rubber bearing (LRB) is used as the isolation device [9, 12–16]. Kawashima and Shoji [16] recommended that the yield force of the LRB can be taken as 10–20% W, while Ghobarah and Ali [12] recommended that the yield force of the LRB can be taken as 5% W, which provides a reasonable balance between reduced forces in the piers and increased forces on abutments. However, in this study, the yield force and yield stiffness of the LRB are taken as 5% W and 5% W/mm, respectively [12]. Given

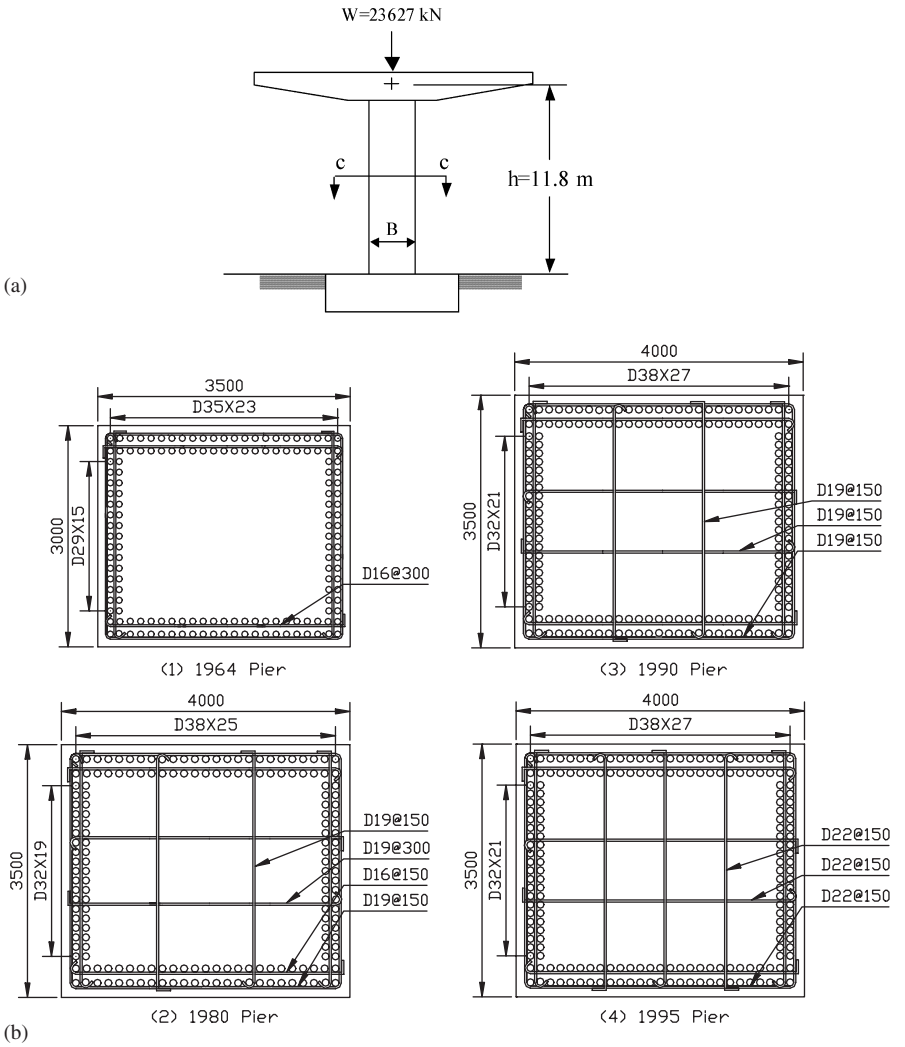

Figure 1. Elevation and sectional views for the four typical bridge piers used in this study. (a) Elevation of a typical bridge pier. (b) Cross-sections at c-c.

the yield force level and the lead yield strength of 10–10.5 MPa [9, 12], the number and cross-sectional area of the lead plugs can be designed. The advantage of the LRB is that it has low yield strength and sufficiently high initial stiffness that results in higher energy dissipation [9, 12–16]. The substructure stiffness for the whole bridge system is given as the sum of the stiffness of all piers [15]. The physical models of the non-isolated and isolated bridge systems are shown in Figure 2. The natural period for the non-isolated system to the longitudinal direction is 0.41 s, and it shifts to 1.24 s for the isolated system, which falls within the practical range of natural period for isolated systems [12, 16].

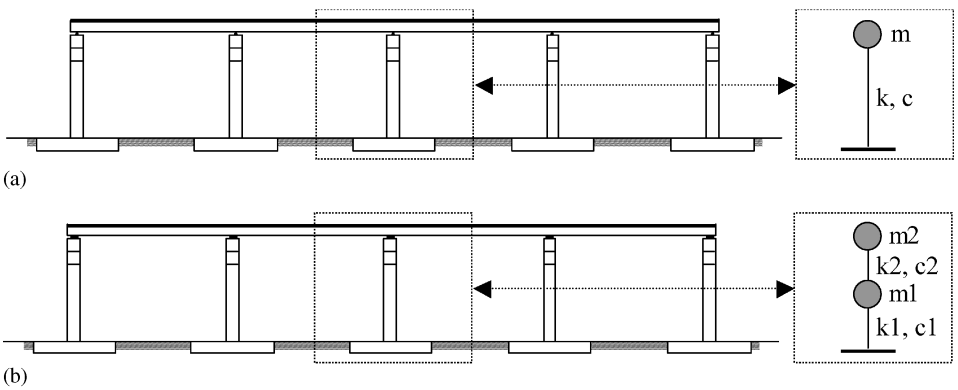

Figure 2. Physical models of the non-isolated and isolated bridge systems used in this study. (a) Physical model of a non-isolated bridge system. (b) Physical model of an isolated bridge system.

INPUT GROUND MOTIONS

For a non-linear dynamic response analysis and to get a wider range of the variation of input ground motion, a total of 250 strong motion records were selected from five earthquake events that occurred in Japan, the United States, and Taiwan. The earthquake events include: the 1995 Kobe, the 1994 Northridge [17], the 1993 Kushiro-Oki, the 1987 Chibaken-Toho-Oki, and the 1999 Chi-Chi [18] earthquakes. Note that the records were selected from all these earthquake events on the basis of larger PGA.

DAMAGE ANALYSIS AND FRAGILITY CURVES

Damage analysis

After performing the non-linear static pushover [19, 20] and dynamic response analyses [21, 22] for the damage assessment of the structure, the Park–Ang [23] damage model was used in this study. For a non-linear dynamic response analysis, the piers and the non-isolated bridge system were modelled as a single-degree-of-freedom (SDOF) system [9], a bilinear hysteretic model was considered [9, 22], and the post-yield stiffness was taken as 10% of the initial stiffness with 5% damping ratio [22]. For the isolated system, a two-degree-of-freedom (2DOF) system [12–16] was modelled, a bilinear hysteretic model was considered for both the substructure and isolation device [12, 16], the post-yield stiffness was taken as 10% of the initial stiffness for both the substructure and isolation device [9, 12, 16], the damping matrix $\mathbf{C}$ was evaluated by using the Rayleigh damping [9, 21], and the damping constant h_i was found by using the following expression [10]

$$h_i = \frac{\sum_{j=1}^{n} h_j \Phi_{ij}^T \mathbf{K}_j \Phi_{ij}}{\Phi_i^T \mathbf{K} \Phi_i} \tag{1}$$

where h_j is the equivalent damping constant of element j, Φ_{ij} is the mode vector of element j of the i-th vibration mode, $\mathbf{K}_j$ is the equivalent stiffness matrix of element j, Φ_i is the mode vector of the overall structure of the i-th vibration mode, and $\mathbf{K}$ is the equivalent stiffness matrix of the overall structure. Using these parameters, the damage to the bridges due to ground motions was obtained by performing a series of both non-linear static pushover [19, 20] and dynamic response analyses [21]. The damage to the bridges was quantified by a damage index DI that is obtained by using the Park–Ang damage model [23], which is then used to construct the fragility curves. The damage index DI is expressed as

$$DI = \frac{\mu_{\mathrm{d}} + \beta \cdot \mu_{\mathrm{h}}}{\mu_{\mathrm{u}}} \tag{2}$$

where μ_{d} and μ_{u} are the displacement and ultimate ductility, β is the cyclic loading factor taken as 0.15, and μ_{h} is the cumulative hysteretic energy [24] ductility. The obtained damage indices for the selected input ground motions were then calibrated to get the damage ratio for each damage rank, which was used to construct the fragility curves [6].

Structural damage and input motion parameters

To construct a relationship between earthquake ground motion and structural damage, a data set comprising inputs (strong motion parameters) and outputs (damage) is necessary. There are two methods for doing this: (i) collect the actual earthquake records and damage data, and (ii) perform earthquake response analyses for given inputs and models and obtain the resultant damage (outputs). The former is more convincing because it uses actual damage data. However, earthquake records obtained near structural damage are few. With the latter, it is easier to prepare well-distributed data. Since it is not based on actual observations, however, much care should be taken in selecting structure models and input motions. The former was used by Yamazaki *et al.* [1] and Tong and Yamazaki [25], and the latter is used in this study.

Selection of input motion parameters to correlate with the structural damage is important, however, it is not an easy task. The Peak Ground Acceleration (PGA) and Peak Ground Velocity (PGV) are commonly used indices to describe the severity of the earthquake ground motion. However, it is well known that a large PGA is not always followed by severe structural damage, especially for long-period structures. Similarly, a large PGV is not always followed by severe structural damage [26], especially for the input motion including permanent fault displacements. Other indices of earthquake ground motion, e.g., Peak Ground Displacement (PGD), time duration of strong motion (T_{d}) [27], spectrum intensity (SI) [28], and spectral characteristics, can be considered in damage estimation [29].

In Japan, the Japan Meteorological Agency (JMA) seismic intensity [30–32] has been used as the most important index for estimating structural damage, identifying affected areas, and preparing for crisis management due to earthquakes [33]. Also, Tokyo Gas Co. Ltd., uses the SI value [28] as the index to shut-off the natural gas supply after a damaging earthquake, and has developed an SI-sensor [28] and a new SI-sensor [34, 35], which monitor both PGA and SI. Hence, it is necessary to know the correlation between the JMA seismic intensity and structural damage with other strong motion parameters. Karim and Yamazaki [36] obtained the correlation between the JMA seismic intensity with other strong motion parameters, and it was found that the JMA seismic intensity shows the highest correlation with both PGA and SI. Similarly, the relationship between the DI and other strong motion parameters are

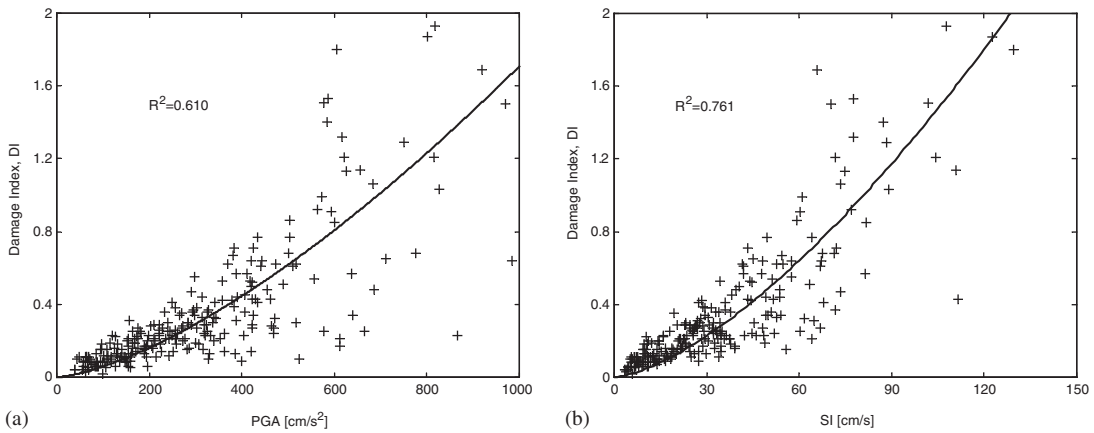

Figure 3. Relationship between (a) damage index and PGA, and (b) damage index and SI obtained from non-linear regression analysis for the 1964 pier.

obtained by performing a non-linear regression analysis [37, 38], and the regression model [25] used in this study is given as

$$y = ax^b \quad \text{(univariate)} \tag{3}$$

$$y = ax^b z^c \quad \text{(multivariate)} \tag{4}$$

where y is the DI, x and z are the strong motion parameters (e.g., PGA, PGV, and SI) and, a, b, c are the regression coefficients. Figure 3 shows the relationship between the DI and PGA, and DI and SI obtained only from univariate regression analysis for the 1964 pier, and the coefficients of determination (R^2) are also shown in the figure. The relationship is also obtained from multivariate regression analysis, and similar to the JMA intensity, it is also found that the DI shows the highest correlation with both PGA and SI ($R^2 = 0.852$). Hence, fragility curves can be constructed with respect to both single and multiple ground motion parameters, however, in this study, only single ground motion parameters are considered, and PGA, PGV, and SI are taken as the amplitude parameters to construct the fragility curves.

Fragility curves

The cumulative probability P_f of occurrence of the damage, equal to or higher than damage rank R, is given as

$$P_f(\geqslant R) = \Phi\left[\frac{\ln X - \lambda_x}{\xi_x}\right] \tag{5}$$

where Φ is the standard normal distribution, X is the ground motion index (e.g., PGA, PGV, and SI), λ_x and ξ_x are the mean and standard deviation of $\ln X$. Two parameters of the fragility curves, i.e., mean λ_x and standard deviation ξ_x are obtained for each damage rank by plotting the damage ratio in each excitation level on a lognormal probability scale, and performing a linear regression analysis. It should be noted that to develop the fragility curves analytically by using Equation (5), the steps given in the 'analytical fragility curves' section

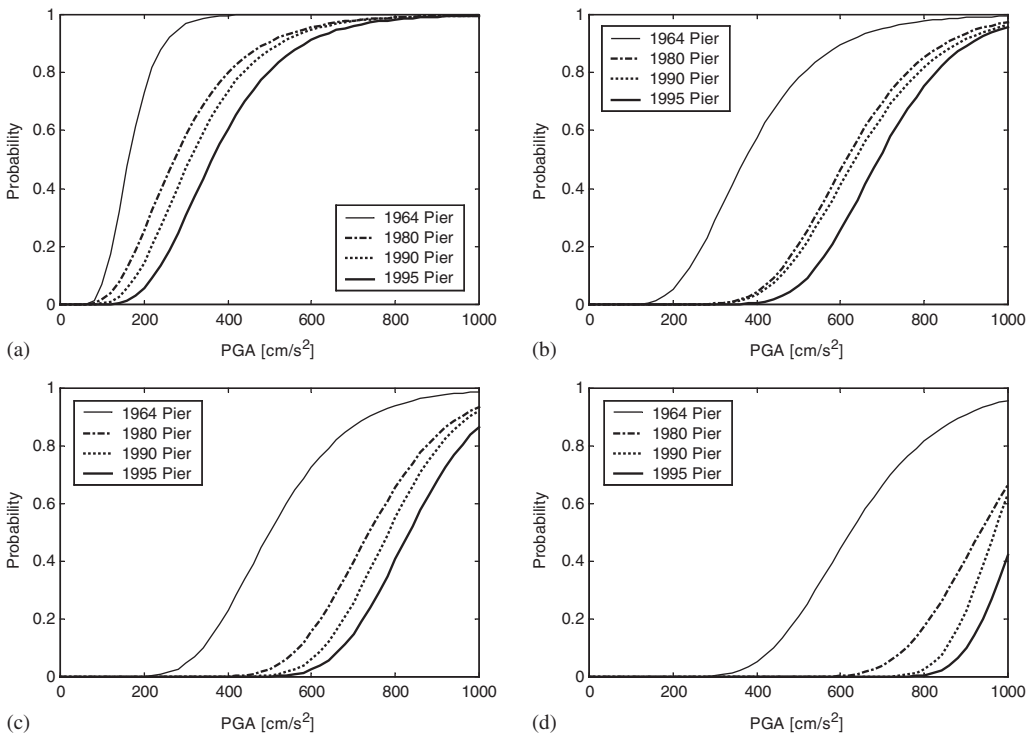

Figure 4. Comparison of the fragility curves for the four bridge piers with respect to PGA. (a) Slight, (b) moderate, (c) extensive, and (d) complete.

are followed here, however, it is highly recommended that one should see Reference [6] for the detailed description of the procedures. It should also be noted that the sole purpose of this study is to develop a simplified method to construct the fragility curves of highway bridges, and the fragility curves obtained by following the approach provided in Reference [6] provide the foundation for developing the simplified method.

Figure 4 shows the plots of the fragility curves for all damage ranks obtained for the four bridge piers with respect to PGA only. One can see that the level of damage probability goes higher from the 1995 pier to the 1964 pier. A similar trend is also observed with respect to PGV and SI, however, it is not shown in the figure. As the code requirements change from time to time (Figure 1(b)), the structure that is designed using the recent code is supposed to perform better against earthquake forces than the previous one, and the evidence for this can be seen in the fragility curves (Figure 4). Figure 5 shows the fragility curves for the non-isolated and isolated bridge systems, and it can be seen that the level of damage probability for the isolated system is less than that of the non-isolated one. A similar trend is also observed with respect to PGV and SI, however, it is not shown in the figure. The lower level of damage probability of the isolated system compared to the one of the non-isolated system is due to the fact that the substructure of the isolated system experiences less lateral forces due to the energy dissipation of the isolation device, which results in the isolation system performing better against seismic forces than the non-isolated system. Now, it is understood

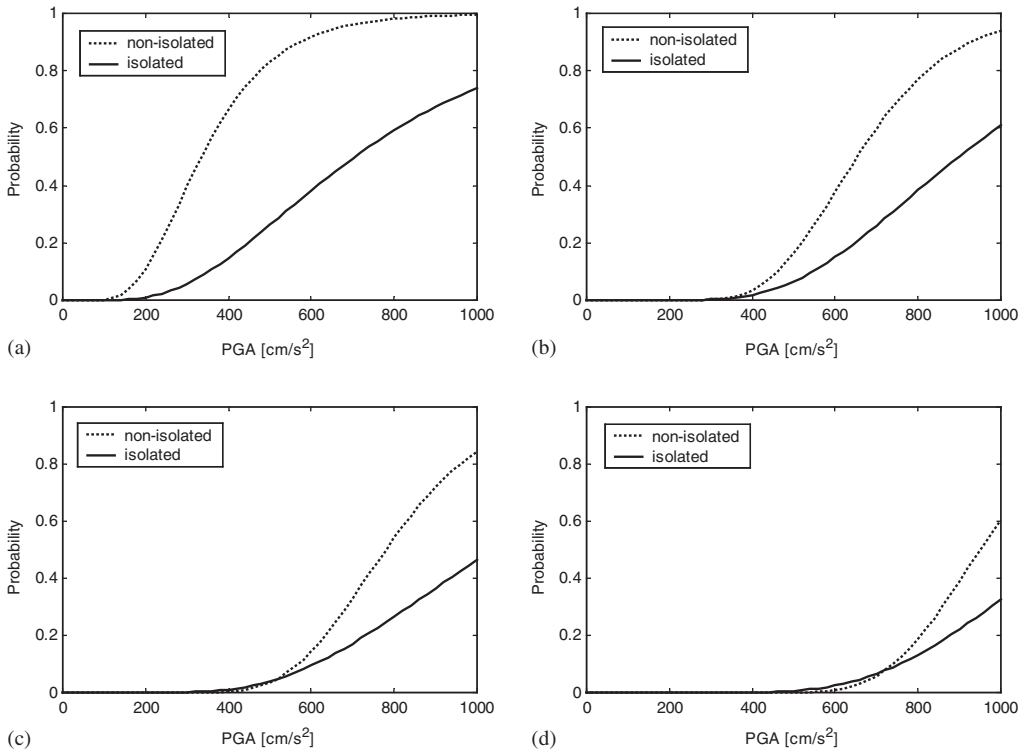

Figure 5. Comparison of the fragility curves for the non-isolated and isolated bridge systems with respect to PGA. (a) Slight, (b) moderate, (c) extensive, and (d) complete.

that there is an effect on the fragility curves (Figures 4 and 5) due to the variation of structural parameters. It is also anticipated that there might be an effect on the fragility curves due to the soil–structure interaction [39], however, this effect is not considered in the present study and further research is necessary.

Relationship between the fragility curve parameters and structural parameters

It is observed from Figures 4 and 5 that if the structural parameters are changed then the fragility curves also change, in other words, there is an effect on the fragility curves due to the variation of structural parameters. However, if one looks at all these fragility curves (Figure 4) then a common trend can be seen among them. As the code requirements change from time to time (Figure 1(b)), so, the structure that is designed using the recent seismic code has a higher strength than the previous one, and it performs better against the seismic forces than the previous one, and the evidence can also be seen on the fragility curves (Figure 4). Hence, it is assumed that there might be a correlation between the fragility curve parameters and the structural parameters, viz., the over-strength ratio θ of the structure, height of the pier (h), span length (L), and weight (W) of the superstructure. However, for simplicity, only θ is considered in the current analysis as it is one of the key structural parameters and provides the information regarding the reserved strength of the structure when it is designed.

The over-strength ratio θ [10] of the structure is defined as

$$\theta = \frac{P_u}{k_{\text{he}} W} \tag{6}$$

where P_u is the horizontal capacity of the structure, k_{he} is the equivalent lateral force coefficient, and W is the equivalent weight, which is calculated as the weight of the superstructure and a 50% weight of the substructure [10]. The lateral force coefficient k_{he} is defined as

$$k_{\text{he}} = \frac{k_{\text{hc}}}{\sqrt{2\mu_{\text{a}} - 1}} \tag{7}$$

where k_{hc} is the design lateral force coefficient, and μ_{a} is the allowable ductility factor [10] of the substructure. The design lateral force coefficient k_{hc} is defined as

$$k_{\text{hc}} = c_{\text{z}} k_{\text{hco}} \tag{8}$$

where c_{z} is the zonation factor, and k_{hco} is the standard design lateral force coefficient. There are mainly three regional classes [10], viz., A, B, and C. A is defined as the region where there is higher earthquake occurrence frequency, while C is defined as the region where there is lower earthquake occurrence frequency. In this study, the region is considered as A, and the corresponding value of c_z for this region is taken as 1.0 [10]. The value of k_{hco} can be obtained knowing the natural period of the structure, and ground condition [10]. In this study, the ground condition is considered as type II.

Note that there are two types of k_{hco}, viz., type I and II. Type I k_{hco} is defined as the design lateral force coefficient stipulated in the earlier Seismic Design Specifications (1990 code), and provides seismic force that hypothesizes a large-scale marine earthquake occurring on the boundary between plates. On the other hand, type II k_{hco} is defined as the design lateral force coefficient stipulated in the recent Seismic Design Specifications (1995 code), and provides seismic force that is based on acceleration strong motion records actually obtained at ground surface during the Hyogo-ken Nanbu (Kobe) earthquake of 1995, and was established by categorizing its acceleration response spectra for each ground category. In this study, k_{hco} is considered as type II. Hence, knowing the natural period of the structure, the standard lateral force coefficient k_{hco} can readily be obtained from the relationship between the standard lateral force coefficient k_{hco} and the natural period of the structure [10].

If one looks at Equations (6) to (8), then it is obvious that the over-strength ratio θ takes into account almost all of the structural parameters, in other words, it is a function of almost all of the structural parameters, viz., ultimate capacity, zonation factor, ground condition, standard lateral force coefficient, structural period, ductility, and weight. It is recommended in the code [10] that the value of θ should be greater than or equal to 1.0, however, the definition for θ is given based on the recent seismic design code [10], and the θ for all the structures are obtained based on this definition irrespective of the design codes that were used to design them. Hence, some values of θ fall below 1.0, especially, for the 1964 pier. The regression model used to obtain the relationship between fragility curve parameters λ and ξ with the over-strength ratio θ is given as

$$\lambda_\theta = b_0 + b_1 \theta \tag{9}$$

$$\xi_\theta = b_0 + b_1 \theta \tag{10}$$

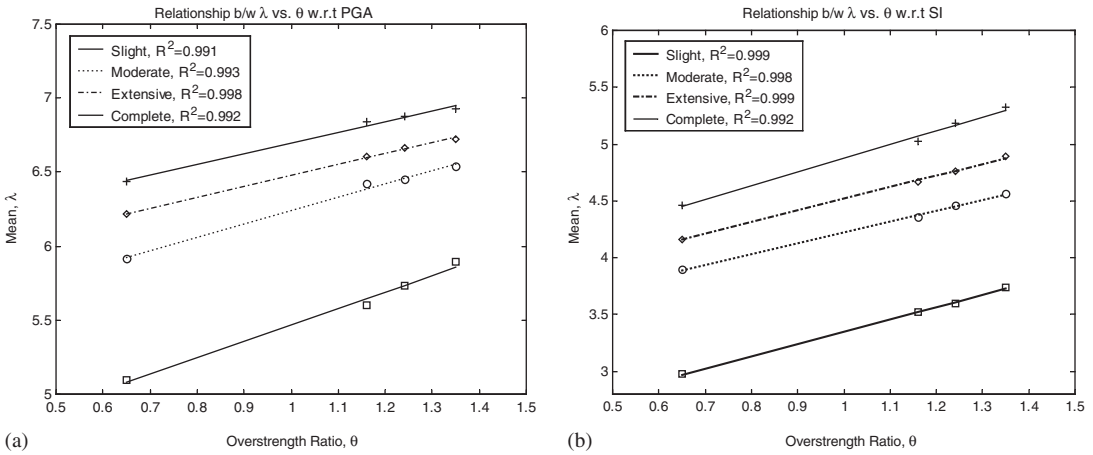

Figure 6. Relationship between fragility curve parameter λ and over-strength ratio θ of the four bridge piers used in this study (a) with respect to PGA, and (b) with respect to SI.

where λ_θ and ξ_θ are the mean and standard deviation of the fragility curves with respect to θ, θ is the over-strength ratio of the structure, and b_0 and b_1 are the regression coefficients.

Figure 6 shows only the relationships between the fragility curve parameter mean λ and the over-strength ratio θ obtained from linear regression analysis for the four bridge piers for all the damage ranks with respect to PGA and SI, and the corresponding coefficients of determination (R^2) are also shown in the figure. Note that the data points for the isolated and non-isolated bridge systems are not included in the regression analysis as they are different systems having different pier height. It can be seen (Figure 6) that there is a very strong correlation between the fragility curve parameter λ and the over-strength ratio θ, and the R^2 values are obtained for the four damage ranks with respect to PGA as 0.991, 0.993, 0.998, and 0.992, respectively, and with respect to SI, the values are obtained as 0.999, 0.998, 0.999, and 0.992, respectively. This clearly indicates that there is a strong correlation between λ and θ, and this relationship may be a very useful tool for constructing the fragility curves for highway bridges knowing the θ factor only.

SIMPLIFIED METHOD TO CONSTRUCT THE FRAGILITY CURVES

Description of bridge models

In the preceding section, it is observed that there is a strong correlation between the fragility curve parameter λ and the over-strength ratio θ of the structure. However, to draw a solid conclusion, it is also necessary to consider many bridge structures that take into account all other structural parameters, for instance, span length (L), pier height (h), weight of the superstructure (W), etc. In this case, a total of 30 bridge models are considered to have a wider range of the variation of structural parameters. The bridges are considered non-isolated, the piers are rectangular, pin-jointed to the superstructure and fixed to the base, and the

Table I. Structural properties for the 30 bridge models used in this study.

Design code	Span length, $L = 35$ m, 40 m ($W = 500$ kN/m)										Reinforcement	
	Pier height (m)											
	6		9		12		15		18		Long.	Tie
	section		section		section		section		section		ρ_l (%)	ρ_t (%)
	a[1]	b[2]	a[1]	b[2]	a[1]	b[2]	a[1]	b[2]	a[1]	b[2]	area ratio	vol. ratio
1964	2.0	2.8	2.6	3.2	3.0	3.5	3.4	3.8	3.5	4.0	1.21	0.09
1980	2.1	3.0	2.8	3.2	3.2	3.8	3.8	4.0	3.8	4.2	1.25	0.32
1995	2.2	3.0	2.8	3.4	3.2	4.0	3.8	4.2	4.0	4.5	1.36	1.03

[1] Dimension in the longitudinal direction in m.
[2] Dimension in the transverse direction in m.
σ'_c (MPa) and σ_{sy} (MPa) are taken as the same for all the codes, and they are taken as 27 and 300, respectively.

superstructure is assumed to slide on ordinary frictionless bearings at the abutments. The ground condition is considered as type II, the regional class is considered as A, and the k_{hco} is considered as type II.

The bridge models are divided into three categories, viz., bridges designed with different seismic codes, bridges having different pier heights, and bridges having different span lengths or weights, however, the number of spans for all the bridge models is assumed to be four. The substructures (piers) for any typical bridge model are considered to be similar; in other words, one pier model can be considered as representative of all other piers for a particular bridge structure. This assumption is adopted to avoid a rigorous computation necessary to perform non-linear pushover analysis for all the piers of a particular bridge model. The physical model is considered as the one shown in Figure 2(a), and the substructure stiffness of the whole bridge system is given as the sum of the stiffness of all piers.

Table I shows all the structural properties for different categories of bridges having span lengths of 30 m and 40 m with superstructure weight of 500 kN/m. Note that the same structural properties have been considered for all the bridge models having a span length of 40 m; in other words, changing only the span length or weight of the superstructure while all the other parameters remain unchanged. It can be seen (Table I) that the pier cross-section changes for different seismic design codes even having the same height, and it changes from smaller to larger from the 1964 code to the 1995 code. It can also be seen from Table I that the pier cross-section also changes due to the changes of pier height even it is designed with the same seismic code, and it changes from smaller to larger from pier height 6 m to 18 m. One can also see that the longitudinal (area ratio) and tie (volumetric ratio) reinforcement also changes for different seismic codes, and the value goes higher from the 1964 code to the 1995 code.

Correlation of λ and ξ with structural parameters for the 30 bridge models

The fragility curve parameters λ and ξ for the 30 bridge models are obtained by performing a series of non-linear static pushover and dynamic response analyses using the selected 250 strong motion records. The over-strength ratio θ is calculated using Equation (6). The relationships between λ and ξ with the over-strength ratio θ only then are obtained using

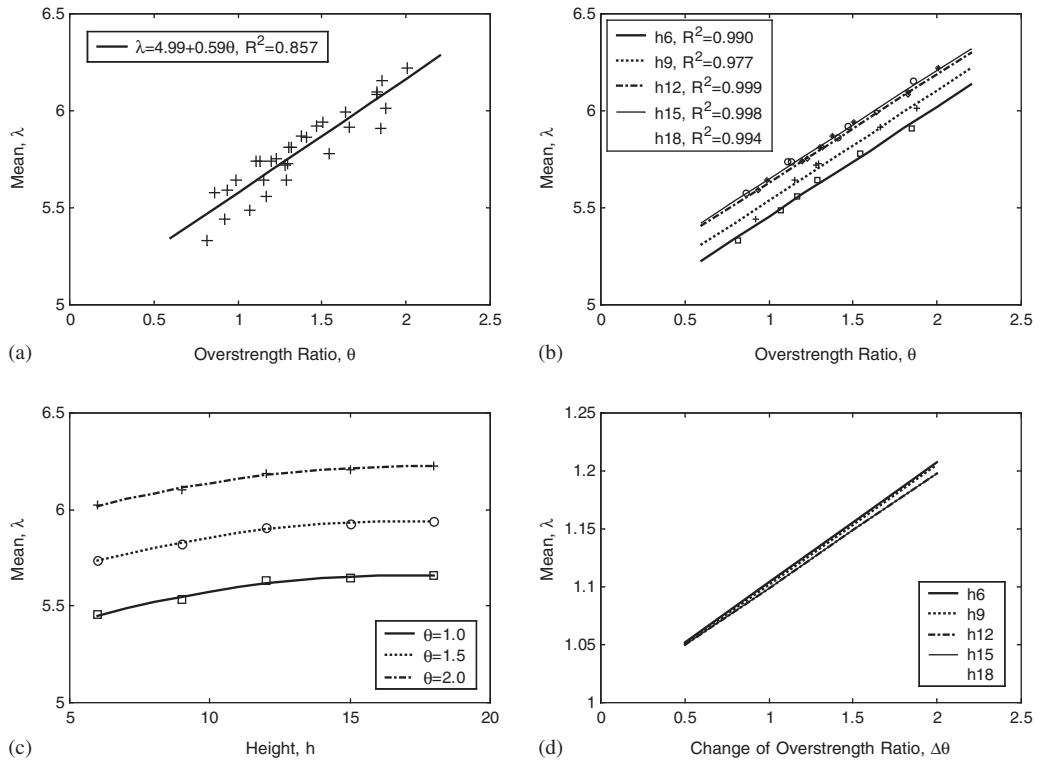

Figure 7. Relationship between (a) λ and θ obtained for the 30 bridge models used in this study, (b) λ and θ for different pier heights, (c) λ and h for different θ, and (d) F_θ and $\Delta\theta$ for different pier heights, all for slight damage with respect to PGA.

Equations (9) and (10) for the all damage ranks with respect to PGA, PGV, and SI considering all the data points obtained for the 30 bridge models.

Figure 7(a) shows the relationship between λ and θ obtained for the slight damage with respect to PGA considering all the data points performing a linear regression analysis. It is observed (Figure 7(a)) that if all the data points are considered together without making any subgroups, for instance, data points for different codes, heights, and weights, etc., then the relationships are found not to be so good as the one found (Figure 6) in the case of the four bridge piers where the heights were the same. Note that the maximum R^2 for both λ and ξ for all the damage ranks with respect to PGA, PGV, and SI is found to be 0.857. It is anticipated that fragility curve parameters might depend on other structural parameters, viz., weight of the superstructure or span length, height of the pier, and variation of the seismic codes even having the same θ value. As the bridge models are grouped mainly in three categories, it is necessary to see how the weight or span length, height of the pier, and different seismic codes influence the fragility curve parameters. In order to do so, the data points are plotted for different pier heights having different superstructure weight or span length, and designed with different seismic codes.

Figure 7(b) shows the plots of λ vs. θ for different pier heights obtained from linear regression analysis, and the corresponding R^2 values are also shown in the same figure. In each level of pier height, the data points are included for different seismic codes and different superstructure weight or span length. It can be seen (Figure 7(b)) that there is a very strong correlation between λ and θ within each level of pier height like the one found (Figure 6) in the case of the four bridge piers where the heights were the same. Although the data points are not plotted for different weights and different seismic codes, as they are included within each pier height, it is clear that there is no significant effect on λ due to the variation of weights and seismic codes. This can be explained in another way: as the θ of the structure is directly related to the weight and ultimate capacity (Equation (6)) of the structure, which is directly related to the seismic code used, the θ takes into account the effect of both weight and the seismic design code used. It is also observed that as the code requirement changes, the θ also changes, which directly influences the λ, and the evidence can be seen in Figures 6 and 7(b), where one can see that the structure that is designed using the recent seismic code has a higher θ value, which results in a higher λ value.

If one looks at all the relationships between λ and θ (Figure 7(b)) obtained for different pier heights, then it can be seen that the relationships are different. These relationships can be used for the bridge structure that has a pier height that is any one of the heights considered in this study. However, practically, the pier height is rather random, and it is not possible to consider a lot of bridge models having a wide range of variation in pier heights due to the limitations of numerical simulation, which could be solved if any stochastic model could be specified to consider the randomness of the pier heights. However, this problem has been solved in another way. First, the λ for different pier heights are obtained by fixing some θ using the relationships shown in Figure 7(b). Then the relationship between λ and h is obtained using the following regression model

$$\lambda_{\mathrm{h}} = b_0 + b_1 h + b_2 h^2 \tag{11}$$

where λ_{h} is the mean with respect to h, h is the height of the pier, and b_0, b_1 and b_2 are the regression coefficients. Figure 7(c) shows the relationship between λ and h obtained for each level of θ. Like the pier height, it is also found that there is a strong correlation between λ and h for different θ, for instance, R^2 is found to be 0.987 for a θ value equal to 1.0. It can be seen from Figure 7(c) that the relationships between λ and h obtained for different θ seem to be quite parallel, and it is also seen that knowing only one of the relationships between λ and h for a given θ, the other relationships for different θ can also be obtained knowing only some scale factors for a change of the θ. In this objective, the scale factors are obtained for changing different θ for different pier heights considering the relationship between λ and h obtained for θ equal to 1.0 as the base one, and the scale factor F_θ is given as

$$F_\theta = a_0 + a_1 \Delta\theta \tag{12}$$

where F_θ is the scale factor with respect to the change of θ, $\Delta\theta$ is the change of θ given as $(\theta - 1)$, and a_0 and a_1 are the regression coefficients.

Figure 7(d) shows the relationship between F_θ and $\Delta\theta$ obtained for different levels of pier heights, and they look very similar. However, to minimize the error that might result for different pier heights, the average scale factor is considered in this study. Hence, the λ value can readily be obtained using Equation (11) for a known h, and then simply multiplying it

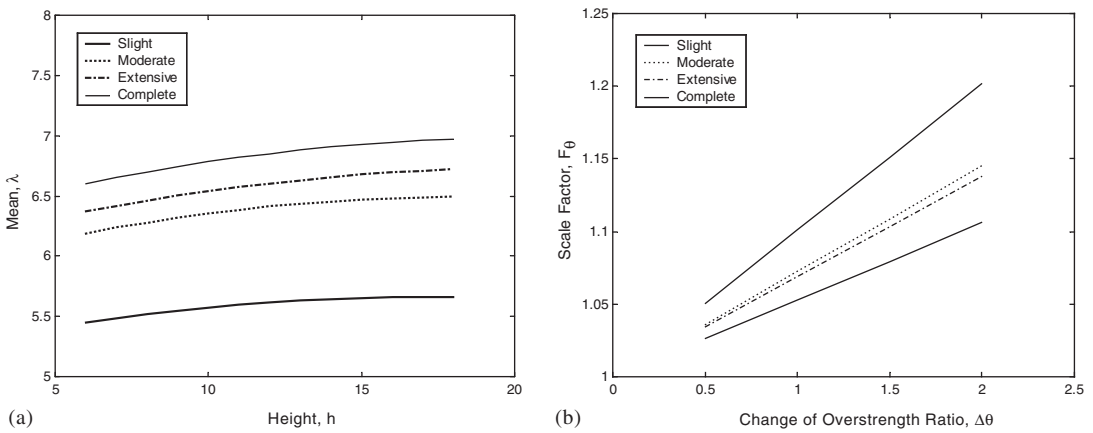

Figure 8. Relationship between (a) λ and h for θ equal to 1.0, and (b) average F_θ and $\Delta\theta$ obtained for different damage ranks with respect to PGA.

by the scale factor F_θ of Equation (12) that can be obtained for a known $\Delta\theta$. In other words, the λ value can be obtained by using the following expression

$$\lambda = \lambda_h F_\theta \tag{13}$$

Substituting for λ_h and F_θ from Equations (11) and (12) into Equation (13) gives

$$\lambda = [b_0 + b_1 h + b_2 h^2][a_0 + a_1 \Delta\theta] \tag{14}$$

From Equation (14), it can be said that λ is a function of both h and θ, and this expression might conveniently be used to obtain the λ for any given h and θ. Similar expressions are also obtained for other damage ranks, i.e., moderate, extensive, and compete. Figure 8(a) shows the relationships between λ and θ obtained for different damage ranks for θ equal to 1.0, and the corresponding average scale factors for λ obtained for different damage ranks are shown in Figure 8(b).

A similar procedure has also been adopted to obtain the expression for standard deviation ξ, and the graphical representation is shown in Figure 9 for a slight damage case. The expression for ξ is given as

$$\xi = [b_0 + b_1 h + b_2 h^2][a_0 + a_1 \Delta\theta] \tag{15}$$

Figure 10(a) shows the relationships between ξ and θ obtained for different damage ranks for θ equal to 1.0, and the corresponding average scale factors for ξ obtained for different damage ranks are shown in Figure 10(b).

Equations (14) and (15) are given with respect to PGA only. Following the same procedure, the expressions for λ and ξ for different damage ranks are also obtained with respect to PGV and SI. Finally, the regression coefficients are obtained for all the damage ranks with respect to PGA, PGV, and SI, and the regression coefficients are shown in Table II. Note that the corresponding R^2 values are also shown in the same table. The simplified expressions (Equations (14) and (15)) obtained for the fragility curve parameters λ and ξ with respect to h and θ may be a very useful tool to construct the fragility curves of highway bridges knowing the

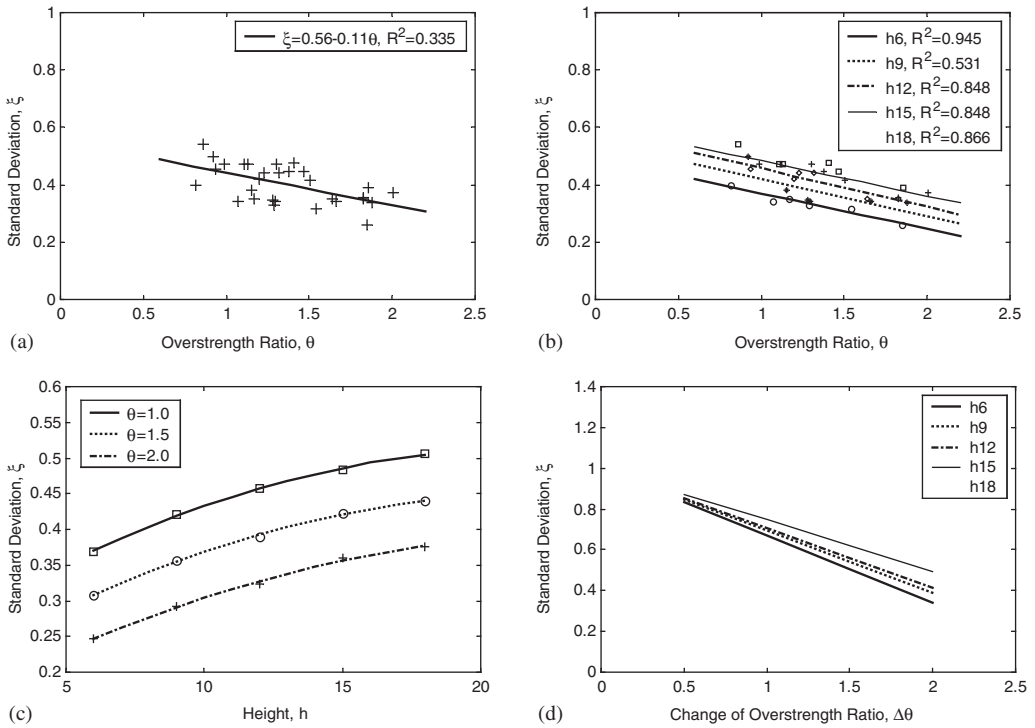

Figure 9. Relationship between (a) ξ and θ obtained for the 30 bridge models used in this study, (b) ξ and θ for different pier heights, (c) ξ and h for different θ, and (d) F_θ and $\Delta\theta$ for different pier heights, all for slight damage with respect to PGA.

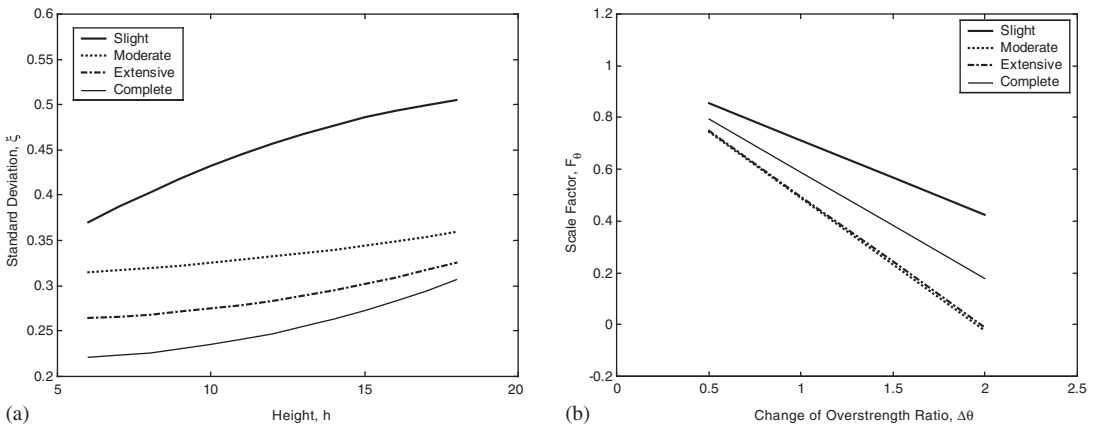

Figure 10. Relationship between (a) ξ and h for θ equal to 1.0, and (b) average F_θ and $\Delta\theta$ obtained for different damage ranks with respect to PGA.

Table II. List of the regression coefficients for the fragility curve parameters obtained from the simplified method.

Indices	DR	Parameters																	
		λ									ξ								
		$\lambda_h = b_0 + b_1 h + b_2 h^2$					$F_\theta = a_0 + a_1 \Delta\theta$				$\xi_h = b_0 + b_1 h + b_2 h^2$					$F_\theta = a_0 + a_1 \Delta\theta$			
		b_0	b_1	b_2	σ	R^2	a_0	a_1	σ	R^2	b_0	b_1	b_2	σ	R^2	a_0	a_1	σ	R^2
PGA	S	5.16	0.06	−0.002	0.014	0.987	1.00	0.07	0.00	1.00	0.24	0.0244	−0.0006	0.002	0.999	1.00	−0.29	0.00	1.00
	M	5.82	0.07	−0.002	0.017	0.991	1.00	0.07	0.00	1.00	0.31	0.0001	0.0001	0.004	0.978	1.00	−0.51	0.00	1.00
	E	6.02	0.07	−0.002	0.021	0.989	1.00	0.05	0.00	1.00	0.27	−0.0021	0.0003	0.003	0.993	1.00	−0.50	0.00	1.00
	C	6.22	0.07	−0.002	0.005	0.999	1.00	0.06	0.00	1.00	0.23	−0.0043	0.0005	0.005	0.991	1.00	−0.41	0.00	1.00
PGV	S	2.84	0.06	−0.001	0.021	0.989	1.00	0.20	0.00	1.00	0.81	−0.0043	−0.0004	0.020	0.955	1.00	0.25	0.00	1.00
	M	3.48	0.11	−0.002	0.045	0.982	1.00	0.18	0.00	1.00	0.72	−0.0095	0.0002	0.004	0.981	1.00	0.44	0.00	1.00
	E	3.55	0.15	−0.004	0.001	0.999	1.00	0.18	0.00	1.00	0.70	0.0002	−0.0002	0.003	0.989	1.00	0.36	0.00	1.00
	C	4.32	0.08	−0.002	0.039	0.975	1.00	0.15	0.00	1.00	0.76	−0.0086	0.0002	0.004	0.981	1.00	0.34	0.00	1.00
SI	S	2.94	0.07	−0.002	0.016	0.989	1.00	0.16	0.00	1.00	0.65	−0.0185	0.0001	0.010	0.991	1.00	0.43	0.00	1.00
	M	3.60	0.09	−0.002	0.025	0.987	1.00	0.16	0.00	1.00	0.51	−0.0160	0.0002	0.006	0.994	1.00	0.99	0.00	1.00
	E	3.73	0.10	−0.003	0.009	0.999	1.00	0.16	0.00	1.00	0.43	−0.0048	−0.0003	0.012	0.974	1.00	0.84	0.00	1.00
	C	3.87	0.14	−0.004	0.031	0.985	1.00	0.19	0.00	1.00	0.33	0.0040	−0.0006	0.009	0.982	1.00	1.28	0.00	1.00

DR: Damage rank, S: Slight, M: Moderate, E: Extensive, C: Complete.

h and θ factors only. It should be noted that the simplified expressions for the fragility curve parameters are obtained based on a set of non-isolated bridge systems, and these simplified expressions for fragility curve parameters might conveniently be used to construct the fragility curves of similar kinds of structures that have similar characteristics. However, these expressions for the fragility curve parameters might be different for isolated bridge systems as the level of damage probability for both the non-isolated and isolated systems was found to be rather different (Figure 5), and it is also anticipated that there might be an effect on the fragility curves due to the soil–structure interaction [39] for which further research is necessary.

Numerical example

To see how the simplified expressions of the fragility curve parameters work, a different bridge structure is considered, which was not used to obtain the simplified expressions. The bridge is designed according to the recent seismic design code in Japan [10]. It is assumed that only the number of spans, span length, superstructure weight, height and cross-section of the pier can be changed while other conditions are the same as those for the 30 bridge models that were used to develop the simplified expressions. For the example bridge structure, the number of spans is assumed to be five, the length of each span is taken as 50 m, the weight is taken as 320 kN/m, the height of each pier is taken as 8 m, and the cross-section of each pier is taken as 2.5 m by 3 m. The over-strength ratio θ is calculated using Equation (6) as 1.32. Now, knowing the height of the pier as 8 m and θ as 1.32, the fragility curve parameters λ and ξ for different damage ranks with respect to PGA, PGV, and SI are obtained using the simplified expressions given in Equations (14) and (15), and using the regression coefficients given in Table II. The λ and ξ are also obtained by performing a series of non-linear static pushover and dynamic response analyses.

Table III. List of the fragility curve parameters for the example bridge structure obtained from both the analytical and simplified methods.

Indices	DR	Parameters					
		λ			ξ		
		Analytical	Simplified	Error, ε (%)	Analytical	Simplified	Error, ε (%)
PGA	S	5.71	5.69	0.26	0.36	0.36	0.00
	M	6.47	6.39	1.13	0.25	0.26	6.26
	E	6.65	6.60	0.76	0.21	0.23	10.31
	C	6.84	6.76	1.22	0.18	0.20	12.06
PGV	S	3.48	3.47	0.27	0.82	0.81	1.40
	M	4.47	4.48	0.29	0.74	0.75	1.03
	E	4.79	4.76	0.80	0.75	0.77	2.31
	C	4.99	5.07	1.45	0.77	0.78	1.27
SI	S	3.52	3.55	0.70	0.62	0.58	6.94
	M	4.40	4.41	0.09	0.49	0.52	7.14
	E	4.66	4.56	2.06	0.46	0.47	1.90
	C	5.03	5.02	0.08	0.42	0.46	10.18

DR: Damage rank, S: Slight, M: Moderate, E: Extensive, C: Complete.

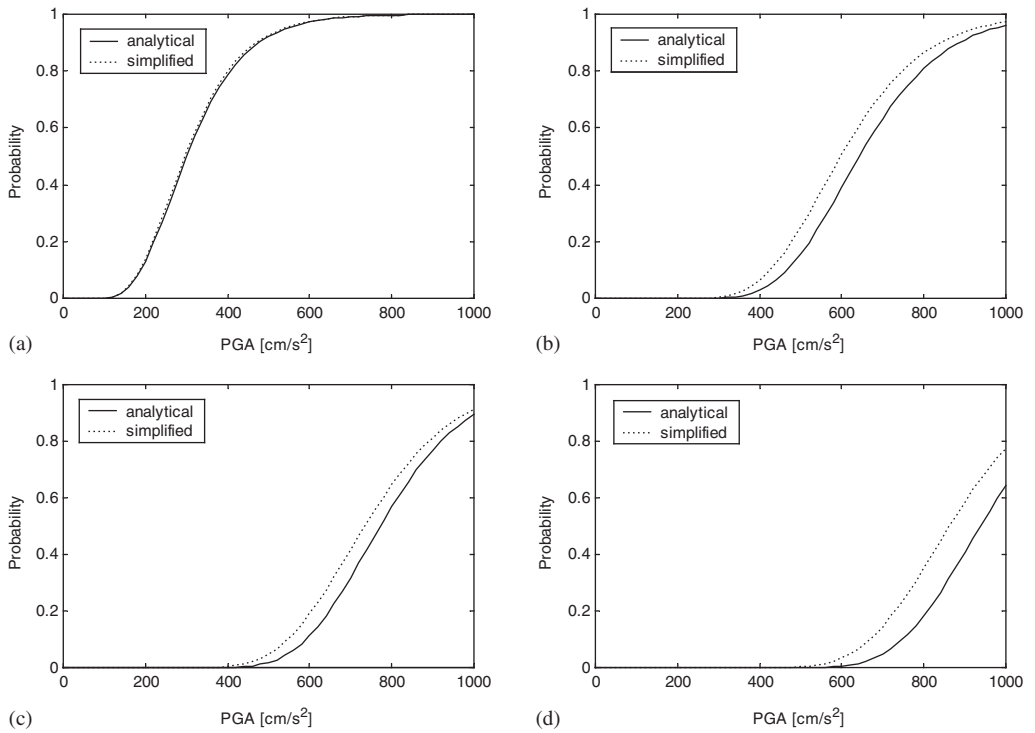

Figure 11. Comparison of the fragility curves obtained from the analytical and simplified methods for a non-isolated bridge system with respect to PGA. (a) Slight, (b) moderate, (c) extensive, and (d) complete.

Table III shows the list of the fragility curve parameters for the example bridge structure obtained from both the analytical and simplified methods, and the corresponding errors ε for the both λ and ξ with respect to the analytical one are also shown in the table. Figures 11, 12, and 13 show the fragility curves for all the damage ranks with respect to PGA, PGV, and SI, respectively, obtained from both the analytical and simplified methods. It can be seen that the fragility curves obtained by both the analytical and simplified methods seem to be very close with respect to PGV (Figure 12), and with respect to SI, they are also found to be very close except for the extensive damage (Figure 13), where a small difference is found. However, with respect to PGA, a small difference is observed for all the damage ranks except for the slight damage (Figure 11).

Note that the maximum errors with respect to PGA, PGV, and SI for both λ and ξ are shown in Table III with an underline mark. It can be seen from Table III that the maximum error for λ with respect to all the parameters, i.e., PGA, PGV, and SI is found to be only 2.06%, and for ξ, it is found as 12.06%. It should be noted that all the values of ξ fall below 1.0 (Table III), and the 12.06% error does not necessarily mean that it might result in a significant difference between the two values, for instance, from Table III, it can be seen that the values of ξ for the analytical and simplified method corresponding to this 12.06% error are found to be 0.18 and 0.20, respectively. Hence, the error terms for both λ and ξ

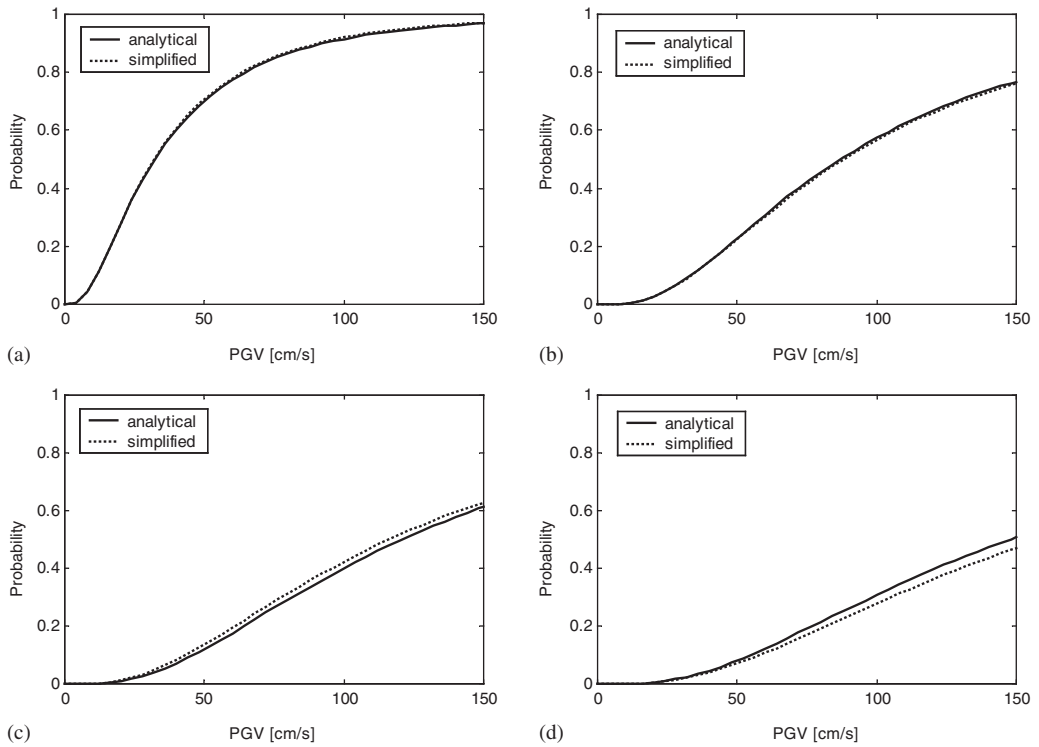

Figure 12. Comparison of the fragility curves obtained from the analytical and simplified methods for a non-isolated bridge system with respect to PGV. (a) Slight, (b) moderate, (c) extensive, and (d) complete.

given in Table III seem to be within an acceptable range, and the simplified method might conveniently be used to construct the fragility curves for non-isolated bridge structures in Japan knowing the height h and over-strength ratio θ only.

CONCLUSIONS

Analytical fragility curves for the four typical bridge piers and two bridge models, (of which one is a non-isolated system and the other is an isolated system) were obtained with respect to the ground motion parameters based on numerical simulation using 250 strong motion records. Based on the non-linear regression analysis between the damage indices of the structure with strong motion parameters, PGA, PGV, and SI were considered as the amplitude parameters for the fragility curves.

It was found that the level of damage probability increases from the bridge pier that was designed by the recent seismic design code to the bridge piers that were designed by the previous seismic design codes, which indicates that there is a significant effect on the fragility curves due to the variation of structural parameters. It was also found that the level of damage

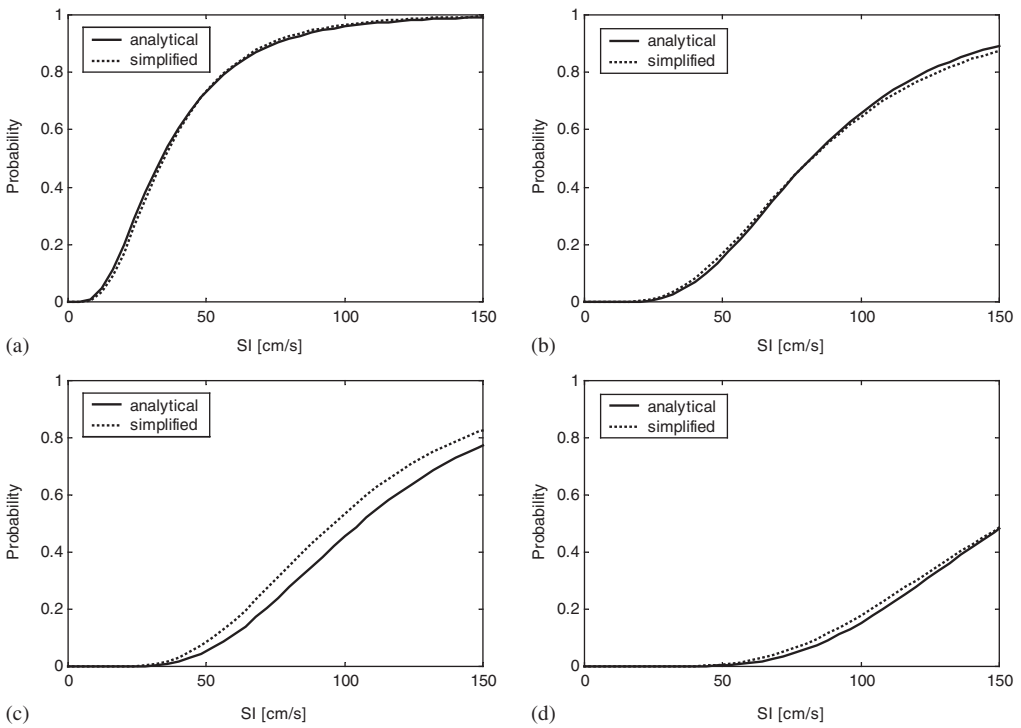

Figure 13. Comparison of the fragility curves obtained from the analytical and simplified methods for a non-isolated bridge system with respect to SI. (a) Slight, (b) moderate, (c) extensive, and (d) complete.

probability for the isolated bridge structure is less than that of the non-isolated one. This is because the substructure of the isolated system experiences less lateral force due to the energy dissipation of the isolation device.

It was observed that fragility curve parameters are highly correlated with the over-strength ratio of the structures. Based on this observation, a simplified method was developed to construct the fragility curves for highway bridges using 30 non-isolated bridge models. The simplified method may be a very useful tool, and conveniently be used to construct the fragility curves for non-isolated bridge systems in Japan knowing the height of the pier and the over-strength ratio of the structure only. The simplified expressions of the fragility curves obtained in this study are expected to be very useful to estimate the level of damage probability for a large number of non-isolated bridges without performing the non-linear static pushover and dynamic response analyses, which fall within the same group and have similar characteristics.

It is anticipated that the simplified expressions of the fragility curves obtained in this study may not be applicable for the isolated systems as the fragility curves for the non-isolated and isolated systems were found to be rather different. It is also anticipated that there might be an effect on the fragility curves due to the soil–structure interaction. Hence, to draw a solid conclusion, it is necessary to consider these two effects for which further research is going on.

REFERENCES

1. Yamazaki F, Motomura H, Hamada T. Damage assessment of expressway networks in Japan based on seismic monitoring. *12th World Conference on Earthquake Engineering*. CD-ROM, 2000; Paper No. 0551.
2. Basoz N, Kiremidjian AS. Evaluation of bridge damage data from the Loma Prieta and Northridge, CA Earthquakes. *Report No. 127*, The John A. Blume Earthquake Engineering Center, Department of Civil Engineering, Stanford University, 1997.
3. Kircher CA, Nassar AA, Kustu O, Holmes WT. Development of building damage functions for earthquake loss estimation. *Earthquake Spectra* 1997; **13**(4):663–682.
4. Ghobarah A, Aly NM, El-Attar M. Performance level criteria and evaluation. *Proceedings of the International Workshop on Seismic Design Methodologies for the next Generation of Codes*. Balkema: Rotterdam, 1997; 207–215.
5. Mander JB, Basoz N. Seismic fragility curves theory for highway bridges. *Proceedings of the 5th U.S. Conference on Lifeline Earthquake Engineering*. TCLEE No. 16, ASCE, 1999; 31–40.
6. Karim KR, Yamazaki F. Effect of earthquake ground motions on fragility curves of highway bridge piers based on numerical simulation. *Earthquake Engineering and Structural Dynamics* 2001; **30**(12):1839–1856.
7. Kawashima K, Sakai J, Takemura H. Evaluation of seismic performance of Japanese bridge piers designed with the previous codes. *Proceedings of the Second Japan-UK Workshop on Implications of Recent Earthquakes on Seismic Risk*. Technical Report TIT/EERG 98-6, 1998; 303–316.
8. Naeim F, Anderson JC. Classification and evaluation of earthquake records for design. *The 1993 NEHRP Professional Fellowship Report*, Earthquake Engineering Research Institute, 1993.
9. Priestley MJN, Seible F, Calvi GM. *Seismic Design and Retrofit of Bridges*. Wiley: New York, 1996.
10. *Design Specifications of Highway Bridges*. Part V: Seismic Design, Technical Memorandum of EED, PWRI, No. 9801, 1998.
11. Sucuoglu H, Yucemen S, Gezer A, Erberik A. Statistical evaluation of the damage potential of earthquake ground motions. *Structural Safety* 1999; **20**(4):357–378.
12. Ghobarah A, Ali HM. Seismic performance of highway bridges. *Engineering Structures* 1988; **10**:157–166.
13. Chaudhary MTA. Evaluation of seismic performance of base-isolated bridges based on earthquake records. *PhD Dissertation*, Department of Civil Engineering, the University of Tokyo, 1999.
14. Chaudhary MTA, Abe M, Fujino Y, Yoshida J. System identification of two base-isolated bridges using seismic records. *Journal of Structural Engineering* (ASCE) 2000; **126**(10):1187–1195.
15. Chaudhary MTA, Abe M, Fujino Y. Performance evaluation of base-isolated bridge using seismic records. *Engineering Structures* 2001; **23**(8):902–910.
16. Kawashima K, Shoji G. Interaction of hysteretic behavior between isolator/damper and pier in an isolated bridge. *Journal of Structural Engineering* (JSCE) 1998; **44A**:213–221.
17. National Oceanic and Atmospheric Administration. *Earthquake Strong Motion CD-ROM*. National Geophysical Data Center, Boulder, 1996.
18. Central Weather Bureau. *Free-Field Strong Ground Data CD-ROM*, Seismological Center, Taiwan, 1999.
19. Bentz EC, Collins MP. Response-2000. *Software Program for Load-Deformation Response of Reinforced Concrete Section*. http://www.ecf.utoronto.ca/~bentz/inter4/inter4.shtml, 2000.
20. SAP2000. *Integrated Structural Analysis and Design Software*, Computers and Structures Inc., 2000.
21. Chopra AK. *Dynamics of Structures*: *Theory and Application to Earthquake Engineering*. Prentice-Hall: Upper Saddle River, NJ, 1995.
22. Kawashima K, Macrae GA. The seismic response of bilinear oscillators using Japanese earthquake records. *Journal of Research*, PWRI, Ministry of Construction, Japan, 1993; **30**:7–146.
23. Park YJ, Ang AH-S. Seismic damage analysis of reinforced concrete buildings. *Journal of Structural Engineering* (ASCE) 1985; **111**(4):740–757.
24. Uang C-M, Bertero VV. Evaluation of seismic energy in structures. *Earthquake Engineering and Structural Dynamics* 1990; **19**:77–90.
25. Tong H, Yamazaki F. A relationship between seismic ground motion severity and house damage ratio. *Proceedings of the 4th US Conference on Lifeline Earthquake Engineering* (ASCE) 1995; 33–40.
26. Loh C-H, Lee Z-K, Wu T-C, Peng S-Y. Ground motion characteristics of the Chi-Chi earthquake of 21 September 1999. *Earthquake Engineering and Structural Dynamics* 2000; **29**:867–897.
27. Trifunac MD, Brady AG. A study of the duration of strong earthquake ground motion. *Bulletin of the Seismological Society of America* 1975; **65**:581–626.
28. Katayama T, Sato N, Saito K. SI-sensor for the identification of destructive earthquake ground motion. *Proceedings of the 9th World Conference on Earthquake Engineering*, vol. 7, 1988; 667–672.
29. Molas GL, Yamazaki F. Neural networks for quick earthquake damage estimation. *Earthquake Engineering and Structural Dynamics* 1995; **24**(4):505–516.
30. Japan Meteorological Agency (JMA) *Shindo wo Shiru* (Note on the JMA seismic intensity). *Gyosei* 1996; 46–224 (in Japanese).

31. Earthquake Research Committee. Seismic activity in Japan-regional perspectives on the characteristics of destructive earthquakes-(excerpt). http://www.hp1039.jishin.go.jp/eqchreng/eqchrfrm.htm, 1998.
32. Shabestari KT, Yamazaki F: A proposal of instrumental seismic intensity scale compatible with MMI evaluated from three-component acceleration records. *Earthquake Spectra* 2001; **17**(4):711–723.
33. Yamazaki F, Noda S, Meguro K. Developments of early earthquake damage assessment systems in Japan. *Proceedings of ICOSSAR'97* (*Structural Safety and Reliability*) 1998; 1573–1580.
34. Shimizu Y, Watanabe A, Koganemaru K, Nakayama W, Yamazaki F. Super high density real-time disaster mitigation system. *12th World Conference on Earthquake Engineering*, CD-ROM, 2000, Paper No. 7.
35. Shimizu Y, Koganemaru K, Yamazaki F, Tamura I, Suetomi I. Seismic motion observed in Taipei basin by new SI sensors and its implication to seismic zoning. *Proceedings of the 6th International Conference on Seismic Zonation*, vol. 2, 2000; 497–502.
36. Karim KR, Yamazaki F. Correlation of JMA instrumental seismic intensity with strong motion parameters. *Earthquake Engineering and Structural Dynamics* 2002; **31**(5):1191–1212.
37. Neter J, Wasserman W, Kutner MH. *Applied Linear Regression Models* (2nd edn). Irwin: Boston, 1989.
38. Draper N, Smith H. *Applied Regression Analysis* (2nd edn). Wiley: New York, 1981.
39. Chaudhary MTA, Abe M, Fujino Y. Identification of soil–structure interaction effect in base-isolated bridges from earthquake records. *Soil Dynamics and Earthquake Engineering* 2001; **21**:713–725.

